A Study on "Through-the-Road"-Parallel-Hybrid Powertrains for Small Aircraft with Distributed Electric Propulsion

Conference Paper · June 2019

DOI: 10.2514/6.2019-3677

4 authors, including:

Philipp Strathoff
RWTH Aachen University
9 PUBLICATIONS **25** CITATIONS

SEE PROFILE

Kai-Uwe Schröder
RWTH Aachen University
197 PUBLICATIONS **1,300** CITATIONS

SEE PROFILE

Eike Stumpf
RWTH Aachen University
149 PUBLICATIONS **969** CITATIONS

SEE PROFILE

A Study on "Through-the-Road"-Parallel-Hybrid Powertrains for Small Aircraft with Distributed Electric Propulsion

Philipp Strathoff[1] and Eike Stumpf[2]
RWTH Aachen University, Aachen, 52062, Germany

Miguel Nuño[3] and Kai-Uwe Schröder[4]
RWTH Aachen University, Aachen, 52062, Germany

Since electrical powertrain components, in particular batteries, do not reach performance levels that allow for the design of small aircraft with meaningful ranges yet, it is worth investigating powertrain architectures other than all-electric configurations in terms of feasibility and suitability as bridge technology. The proposed powertrain concept features a combustion engine driving a nose-mounted cruise propeller as well as an all-electric active lift augmentation system realized by high-lift propellers distributed along the main wing's leading edge. Performance of this aircraft configuration is evaluated by the Institute of Aerospace System's in-house aircraft conceptual design and evaluation environment MICADO. A comparison with a generic conventional single engine reference aircraft, sized towards the same top-level aircraft requirements and design specifications, reveals that the proposed powertrain concept makes fuel savings of up to 8% possible. If additional electric energy consumption is considered, overall primary energy consumption can be decreased by up to 7%.

I. Introduction

In recent years, substantial effort has been dedicated to the development of aircraft with all-electric powertrains. This is particularly true for general aviation-class aircraft. All-electric powertrains promise enhanced efficiency from tank respectively battery to propeller due to the high efficiency of electric components. In addition, the rather free scalability of electric motors opens up new and more efficient aircraft design options. Regarding small, general aviation-class aircraft, NASA has been investigating the concept of distributed electric propulsion for several years and as part of the SCEPTOR [1] project a flight demonstrator, the X-57 Maxwell, is actually built. The aim is to demonstrate a fivefold efficiency increase compared to cruise flight performance of the conventionally powered TECNAM P2006T by using all-electric propulsion and increasing aerodynamic efficiency. Several high-lift propellers attached to the X-57 wing's leading edge accelerate the flow over the wing at low airspeeds. This allows for a smaller wing with a higher wing loading. In case of the X-57, wing aspect ratio is increased as well. By these modifications aerodynamic efficiency during cruise flight, which is usually the longest mission segment, can be significantly increased. The distribution of propulsive power to several units means that the individual engines are comparatively small. In terms of efficiency, maintenance and economic aspects this is only meaningful for electric motors but not for combustion engines making an at least partially electrified powertrain inevitable. However, currently available battery technology still prevents aircraft designers from building all-electric aircraft with flight ranges comparable to those of conventionally powered aircraft. Heavy batteries limit the range and payload of all-electric aircraft drastically.

[1] Researcher and PhD student, Institute of Aerospace Systems (ILR)
[2] Head of institute, Institute of Aerospace Systems (ILR)
[3] Researcher and PhD student, Institute of Structural Dynamics and Lightweight Design (SLA)
[4] Head of institute, Institute of Structural Dynamics and Lightweight Design (SLA)

Based on an investigation of four-seat all-electric aircraft, Kreimeier [2] suggests that a minimum battery specific energy density of 400 Wh/kg is necessary to design small aircraft for on-demand air mobility with ranges above 250 NM. In a report from Roland Berger [3] the figure of 500 Wh/kg is stated as broadly accepted minimum for electrical storage systems in aviation applications. Hepperle [4] concludes that based on a battery energy density of 150-200 Wh/kg at least a five to tenfold increase in energy density is necessary to build commercially attractive regional aircraft. The figures stated before often correspond to battery energy density at pack level. In order to build battery packs with those energy densities, a considerably higher specific energy density at battery cell level is necessary. This is due to packaging material, elements for ensuring crashworthiness and battery cooling which all add further extra weight to the battery pack. While current state-of-the-art cells achieve energy densities of 200-250 Wh/kg, energy densities of around 400 Wh/kg will probably not be reached before 2030 [5].

In contrast to all-electric propulsion, hybrid-electric propulsion is often referred to as a meaningful intermediate step towards all-electric flight. Several different hybrid-electric powertrain architectures can be identified. On a high level, serial- and parallel-hybrid as well as serial-parallel (or mixed) powertrain architectures can be distinguished. In a serial-hybrid configuration, propellers are solely driven by electric motors, which are supplied with electricity by a generator attached to an internal combustion engine. Most often, a battery is added to the powertrain to buffer peak power demand. This layout leaves the designer to a large extent the design flexibility of all-electric powertrains while, at the same time, increased ranges and payload are possible due to the use of hydrocarbon fuels as main energy source. However, the dual energy conversion from fuel to mechanical energy and then from mechanical energy to electric energy is less efficient than a single energy conversion.

In contrast to serial-hybrid powertrains, parallel-hybrid powertrains avoid the dual energy conversion. They appear in two different layouts. On the one hand, both a conventional engine and an electric motor can be directly connected to a propeller shaft via a gearbox. On the other hand, some propellers can be driven by combustion engines while others are driven by electric motors. In automotive context, the latter architecture is referred to as "Through the Road"-Parallel (TTR-parallel). In a TTR-parallel layout, there is no link between conventional and electrical powertrain.

Because of their complexity and the mass sensitivity of aircraft, most other forms of hybrid-electric powertrain architectures are often not feasible for application in aircraft. An overview on the before described powertrain layouts ranging from conventional to hybrid-electric and all-electric designs is given in Fig. 1.

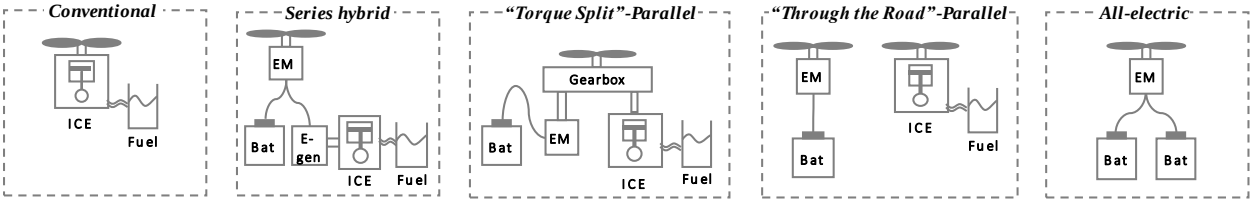

Fig. 1 Layouts of conventional, hybrid-, and all-electric powertrains

Although NASA's X-57 Maxwell aircraft is a generally promising concept, there are at least two reasons to investigate variations of this concept. First and as already mentioned before, in the near future a full-electric powertrain is infeasible for aircraft with ranges of several hundred nautical miles due to heavy batteries. This can be remedied by using a hybrid-electric powertrain. Second, the large tip-mounted cruise propellers are likely to cause directional stability problems in case of one engine inoperative. In addition, ground clearance for avoidance of wing tip strikes can hardly be ensured. While tip-mounted propellers allow for induced drag reduction if rotating in opposite direction compared to the tip vortex, this efficiency increasing effect can no longer be used if propellers are placed elsewhere.

Having in mind the limitation of both range and payload of all-electric aircraft, powertrain architectures other than all-electric for small aircraft with distributed electric propulsion, which is used as a synonym for active lift augmentation through high-lift propeller-wing-interaction in the context of this paper, could be a solution to this problem. Regarding variations of the powertrain architecture for an aircraft with distributed propulsion technology, an analysis of the layouts displayed in Fig. 1 reveals that the number of possible powertrain layouts is limited. This is due to the small size of distributed power units and the associated low efficiency of small combustion engines. In addition to an all-electric powertrain, a serial-hybrid architecture is feasible because all propellers can be driven by electric motors while the electricity is supplied by an internal combustion engine attached to a generator sitting inside the fuselage. This configuration has already been investigated by Kreimeier [2]. His results show that small degrees of hybridization, i.e. small amount of flight energy originating from batteries, are beneficial. With respect to hybrid-parallel architectures, only the TTR-parallel layout is meaningful aircraft with distributed electric propulsion as it allows some propellers to be driven by electric motors while others are powered by combustion engines. Regarding

"Torque Split"-parallel layouts, no meaningful configuration featuring a conventional engine and an electric motor on the same high-lift propeller shaft could be identified for aircraft with high-lift propellers. As a result, the application of a TTR-parallel powertrain to a small aircraft is investigated in more detail. The TTR-parallel powertrain layout allows using the aerodynamic benefits associated with distributed electric propulsion for lift augmentation while overall aircraft mass can be kept low due to the use of hydrocarbon fuel as major source of energy.

Starting from an aircraft design similar to NASA's X-57 Maxwell aircraft, the two cruise propellers are detached from the electric powertrain, reduced to one propeller and attached to a conventional piston engine. This engine is placed in the aircraft nose. The active DEP high-lift system remains powered by batteries as it is used only for a couple of minutes during each mission. Even though thrust generation of the DEP system is not desired, it cannot be avoided when high-lift propellers are operated. For that reason, it is examined whether the size of the cruise engine can be reduced to meet cruise power demand while the active DEP system is sized to 1) provide the necessary high-lift and 2) the thrust difference between the thrust of the cruise propeller and the required maximum (takeoff) thrust on the other hand. A notional design of the proposed aircraft concept is shown in Fig. 2.

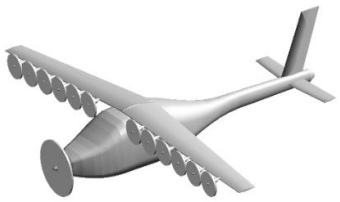

Fig. 2 Notional design of the proposed aircraft concept with DEP and hybrid TTR-parallel powertrain

II. Aircraft design methodology

The study is carried out with the Institute of Aerospace Systems' (ILR) Multidisciplinary Integrated Conceptual Aircraft Design and Optimization environment MICADO. As a result of a major extension described in [2], MICADO, which was originally developed for design, evaluation and optimization of civil transport aircraft [6], is now capable of modeling both airliners and general aviation-class aircraft. The functional structure of the MICADO design and sizing process is shown in Fig. 3. Based on a given set of top-level aircraft requirements (TLAR) and design specifications, the design process starts with an *initial sizing* where thrust-to-weight ratio (T/W, resp. power-to-weight ratio P/W) and wing loading (W/S) are determined based on a constraint analysis. After that, a detailed aircraft component sizing and performance analysis is iteratively repeated until convergence criteria for aircraft parameters, such as maximum takeoff mass and block fuel consumption, are met. An integrated parameter study manager enables the user to study the influence of changes to input values, such as design parameters and mission profile, on the overall aircraft design, performance, economics and ecological impact. Due to the modular based software architecture, individual modules can be easily extended or exchanged.

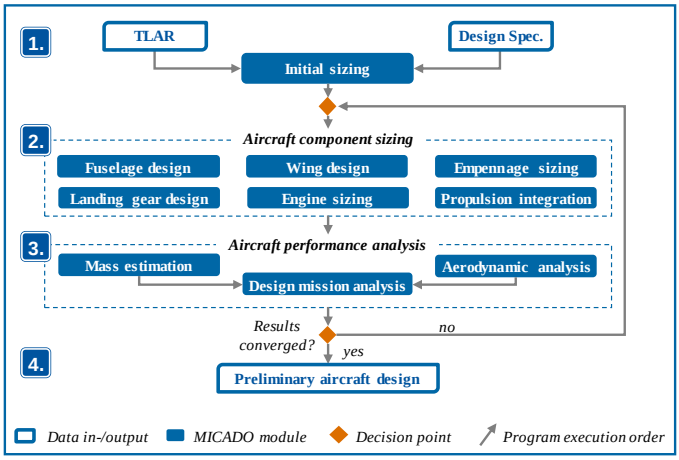

Fig. 3 Functional structure of the MICADO design process

Regarding aircraft with distributed electric propulsion, a proper consideration of aerodynamic propeller-wing-interaction is indispensable. This is particularly true if DEP is used for lift augmentation. Within the current MICADO

environment, this interaction is considered by superposition of clean wing aerodynamics and high-lift propeller slipstream. First, lift and induced drag of the clean wing configuration are calculated by using the German Aerospace Center's (DLR) Lifting_Line [7, 8] software. Second, high-lift propeller induced velocity is calculated for a predefined set of flight and high-lift propeller operating conditions characterized by airspeed, aircraft angle of attack, altitude, propeller speed and propeller input power. For each combination, induced velocity in the propeller slipstream is calculated using a combination of the blade element and momentum theory (BEMT). During execution of BEMT, the presence of a wing behind the high-lift propellers is neglected. The impact of high-lift propeller operations is summarized in a dynamic pressure multiplier that indicates the factor by which dynamic pressure at the wing increases during operation of high-lift propellers. The installation position of the high-lift propellers relative to the wing as well as the contraction of the propeller wake dependent on installation position and operating condition are considered. Dynamic pressure multipliers for the above-mentioned set of operating conditions are summarized in a look-up table called "prop-wing-interaction-map". Within the *mission analysis* tool, the prop-wing-interaction-map is used to determine lift and drag of the aircraft during high-lift propeller operation by interpolation between tabulated operating conditions. A more detailed description of this method and the corresponding fundamentals can be found in [2, 9, 10].

The technical design of the active lift augmentation system, i.e. the sizing of system components, such as high-lift propellers and electric motors, can be controlled by changing the parameter *design maximum high-lift coefficient* $C_{L,max,DEP}$. In assumption of a constant stall speed of v_{stall} = 61 kn for every aircraft, the minimum wing area is determined following Eq. (1) where S is wing area, W is aircraft weight, and ρ_{SL} is air density at sea level.

$$S = \frac{W}{c_{L,max}^{DEP} \cdot \frac{1}{2} \rho_{SL} v_{stall}^2} \tag{1}$$

Based on the difference between the design maximum high-lift coefficient $C_{L,max,DEP}$ and the maximum high-lift coefficient of the wing that can be achieved without using DEP, the components of the active lift augmentation system are sized. It is assumed that all high-lift propellers and their driving motors are identical within one aircraft design. A detailed description of this part of the sizing process can be found in [2].

A. Hybrid-parallel powertrain sizing

Design and sizing methodologies regarding the hybrid-parallel powertrain components include a component sizing towards meeting both propulsive power and mission energy requirements as well as estimating dimensions and masses of the individual components. Regarding conventional powertrains for combustion engines, considered powertrain components from tank to propeller include components such as fuel tanks, combustion engine, and propeller. For electric powertrains components such as batteries, cables, controllers, inverters, electric motors, and propellers are considered.

The component sizing strategy is closely linked to the operational strategy during the mission. Typically, most components run most efficiently if they operate constantly in close proximity to their design point. The cruise segment is usually the longest part of a mission. In contrast to conventional aircraft configurations, which require the engine to meet peak power demand, the combustion engine in the TTR-parallel powertrain can be sized to meet cruise flight conditions in order to achieve a low consumption of hydrocarbon fuel. From takeoff to top of descent, the combustion engine in the TTR-parallel powertrain is operated on a level as constant as possible. Additional power or rather thrust is delivered by the electric motors of the active high-lift system. However, the operational strategy is to operate the electric motors only if necessary. This means a support of the cruise flight is to be avoided. By doing so, the flow around the wing during cruise flight is disturbed by high-lift propeller nacelles only (high-lift propeller blades are assumed foldable) and not additionally by high-lift propeller operations. Moreover, short operating time of electric motors keeps heavy batteries smaller.

The sizing of the powertrain begins within MICADO's *initial sizing* module where a power-to-weight ratio is estimated based on the outcome of a constraint analysis. This ratio is usually kept fix throughout the entire sizing loop. Further powertrain component sizing steps are carried out within the *engine sizing* and *propulsion integration* modules. By multiplication of the power-to-weight ratio with the actual aircraft mass, the required amount of installed overall engine power can be obtained. In case of a TTR-parallel architecture, this overall power is divided between the two different powertrain types in the next step.

$$P_{tot} = \frac{P}{W} \cdot W = P_{conv} + P_{el} \tag{2}$$

Since specific power of electric motors is significantly higher than that of combustion engines, the combustion engine is sized as small as possible while ensuring that it can deliver enough power to propel the aircraft solely throughout the entire cruise flight. This can be achieved by solving Eq. (3).

$$P_{comb} = \frac{D \cdot v_{cr}}{\eta_{prop}} = \frac{L \cdot v_{cr}}{\eta_{prop} \cdot L/D} = \frac{m \cdot g \cdot v_{cr}}{\eta_{prop} \cdot L/D} \quad (3)$$

Combustion engine shaft power P_{comb} can be obtained by dividing propulsive power by the propeller's propulsive efficiency η_{prop}. In constant cruise flight, propulsive power equals the product of drag D times cruise speed v_{cr}. Expanding the equation by lift L yields the glide ratio L/D and allows the introduction of aircraft mass m as lift equals weight in constant cruise flight. In order to estimate required engine power to the safe side, fuel burn must be taken into account as it leads to a reduction in aircraft mass and thus glide ratio (assumption of constant speed and altitude) over the duration of the mission. Therefore, engine shaft power P_{comb} is calculated by using maximum takeoff mass and the smallest value for glide ratio, which is determined during the cruise part of the mission. Moreover, an average cruise propeller efficiency of 80% during cruise flight is assumed.

The power of each electric high-lift motor is calculated by equally distributing the remaining overall aircraft power (P_{tot}-P_{comb}) over all high-lift motors. In case the amount of remaining power is not sufficient to achieve the specified high-lift coefficient, the algorithm automatically increases high-lift motor power until the high-lift coefficient specification is satisfied.

Some assumptions need to be made regarding the estimation of the mass of the individual powertrain components. Since the aim of this study is the investigation of a technical solution being ready for application in the near future, assumptions on technological parameters are made realistically rather than optimistically. As mentioned before, battery mass is a main driver of overall aircraft mass because their gravimetric energy density (currently around 200-250 Wh/kg) compares poorly to that of hydrocarbon fuels (around 12,000 Wh/kg). According to the battery model's level of detail which describes the battery at pack level, battery mass is determined at pack level by multiplication of battery capacity (in kWh) and a gravimetric energy density constant. This constant is assumed to have the value 250 Wh/kg. Similarly, battery volume on pack level is calculated by multiplying battery capacity and a volumetric energy density constant (300 Wh/L [5]). The mass of combustion engines and electric motors is determined similarly by dividing the engine or motor power by a power density constant. Regarding combustion engines, this constant is assumed to have the value 1.1 kW/kg [11] while the constant's value for electric motors is assumed to be 3.0 kW/kg.

B. Consideration of lift drop due to wing-mounted high-lift propeller nacelles

Mounting nacelles for high-lift propellers directly at or close to the wing's leading edge self-evidently results in a disturbed flow around the wing. This happens not only during operations of the high-lift propellers but also if these propellers are folded away during cruise flight. As a result, drag increases and in addition, lift produced by the wing drops. The effect of dropping lift can be seen in a NASA study on the X-57 wing by Deere et al. [12] who used high-fidelity CFD methods. Results for the wing with high-lift nacelles show a lift coefficient decreased by around ΔC_L=0.1 over the whole angle of attack range compared to the same wing without high-lift nacelles. Other than that, no relevant data on this effect, obtained neither from experiments nor CFD calculations, could be found in the literature. However, the magnitude of this lift drop clearly points to the need of considering this effect during the aircraft design and evaluation process. Otherwise, performance of aircraft using lift augmentation through DEP would be overestimated. Regarding additional drag due to high-lift propeller nacelles on the wing, two aspects need to be taken into account. On the one hand, viscous drag and form drag increase due to increased wetted area. On the other hand, induced drag rises as lift distribution becomes less favorable.

Within MICADO, overall aircraft aerodynamics is calculated in the *aerodynamic analysis* module. As an aircraft conceptual design and optimization environment like MICADO is designed for fast evaluation of different concepts by performing parameter studies, computational speed is a crucial prerequisite. Therefore, not high-fidelity CFD methods but lower order models like panel or vortex lattice methods need to be employed. Currently, the German Aerospace Center's (DLR) software Lifting_Line [8, 7] is used within MICADO to calculate lift and induced drag of the clean wing and stabilizer. Being based on a multiple lifting line method, DLR's Lifting_Line software reduces voluminous wings with appropriate thickness to flat surfaces defined by span and airfoil camber line. For this reason, drag components other than lift-induced drag cannot be calculated. Moreover, disturbances caused by components, e.g. mounted on the wing, cannot be considered. Consequently, without application of any other models or modifications to MICADO's existing *aerodynamic analysis* module, a proper consideration of lift drop and thus increased drag due to high-lift propeller nacelles is not possible. In contrast to Lifting_Line, panel method-based

aerodynamic calculation tools can take into account thickness of aircraft components. However, preliminary studies with the panel code included in OpenVSP [13] did not deliver satisfactory results when applied to the X-57 model in the openVSP database and compared to the afore mentioned results from Deere et al [12].

In order to meet the challenge of aligning the fidelity level of available aerodynamic prediction methods for conceptual aircraft design with the necessary consideration of disturbing effects of wing-mounted high-lift propeller nacelles, a simple modeling approach is applied. As a first approximation, the influence of high-lift propeller nacelles is modeled by putting a penalty on lift production performance of the main wing: First, clean wing aerodynamics, i.e. lift and induced drag, for the main wing and the horizontal stabilizer are calculated with Lifting_Line. Second, a parallel downshift of the main wing's lift polar is applied to model the lift drop due to the nacelles. The parallel shift ΔC_L can be controlled as input parameter during the design and sizing process to study sensitivities. A change of the main wing's lift also results in changes of the aircraft's pitching moment. In order to keep the design logic as consistent as possible, Lifting_Line outputs regarding the pitching moment behavior are corrected. This is done by recalculating the aircraft's pitching moment coefficient for all investigated angles of attack by using the modified lift coefficient of the main wing. In contrast to the pitching moment, changes of induced drag due to less overall lift on the one hand and the disturbed flow around the wing near high-lift propeller nacelles on the other hand are neglected at this stage.

C. Wing mass estimation methodology

Mass estimation methods for aircraft components other than those described above (most notably combustion engines, electric motors and batteries) are mostly taken from Nicolai [14] and Raymer [15]. As described in [2], for all components but the wing the average result of Raymer's and Nicolai's class II equations are used. Since wing mass estimation methods provided by Nicolai and Raymer do not explicitly consider any engines mounted to the wing, it was decided to include a class II & 1/2 wing mass estimation method developed in-house at RWTH Aachen University's Institute of Structural Mechanics and Lightweight Design.

1. Program description

The Aircraft Structural Design Toolbox (ASDT) is a program written in MATLAB used to perform preliminary sizing of main aircraft structural components during the first design phases according to static strength criteria. Buckling and aeroelastic effects are not accounted for during sizing. At first, a stick beam model of the considered aircraft is generated and aerodynamic loads are calculated with a modified version of AVL [14] using the vortex lattice method. Then, the inner loads in the structure are calculated taking aerodynamic, mass and other loads such as thrust into account. These inner loads are then used to dimension each section of the discretized beam structure. Since the structural masses and inner loads depend on the section thicknesses, several iterations updating the masses and resizing each section are performed until mass convergence is achieved. To calculate the total structural mass, the primary structural mass, which results from the static dimensioning, is multiplied with a constant factor to account for secondary and non load-carrying components.

For the calculations done in this paper, several load cases according to the CS-23 specification [15] are considered: maneuvering with maximal and minimal load factor, positive gusts and control deflection loads at maneuvering (v_a) and dive speed (v_d). The wing is discretized in 39 sections evenly distributed along the span. The cross sections are assumed to consist of a torsion-carrying skin, a shear force-carrying web and normal stress-carrying caps at 30% chord.

2. Mass estimation validation

To validate the structural mass estimation methodology, five different aircraft with published structural masses [16] were modelled and sized using ASDT. In Fig. 4, the real values (marked as Roskam) as well as the calculated with class II (Raymer, Nicolai) and class II & 1/2 methods (ASDT) can be seen. The mean difference between the masses calculated with ASDT and the real values from the literature is 6 %, a value slightly smaller than the differences when using class II methods (10 % and 12 %). Since the mass data used for validation consists of 40 to 50 years old aircraft, the calculated value with ASDT is further scaled with a fudge factor (ASDT value scaled) to account for technological improvements such as the use of fiber-reinforced plastics in the structure.

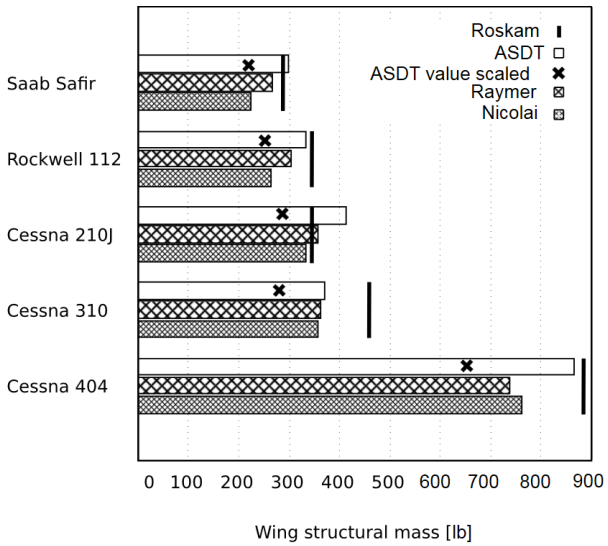

Fig. 4 Real wing structural masses (Roskam) and values calculated using different estimation methods (ASDT, Raymer, Nicolai).

D. Description of aircraft baseline configuration and design mission

The proposed TTR-parallel powertrain architecture is applied to a generic aircraft which features a tadpole-style fuselage, a high wing and a conventional tail in the baseline configuration. Like NASA's X-57 aircraft, the aspect ratio of the wing is assumed to have the value 15. Similar to several other small aircraft, the generic aircraft concept is designed to carry up to four persons including the pilot. In the baseline configuration, there are six high-lift propellers mounted to the leading edge of each side of the main wing. The high-lift propellers are foldable in order to reduce drag during cruise flight when they are not used. The design maximum high-lift coefficient is chosen as $C_{L,max,DEP} = 3.5$. This lift coefficient can only be achieved when high-lift propellers are activated. In addition to the active high-lift system, the wing is equipped with a simple trailing edge flap. The landing gear is assumed to be non-retractable.

All aircraft are designed for the same generic design mission. This baseline design mission is characterized by an assumed design range of 650 NM when carrying 800 lb payload. This is assumed to comprise four persons including light baggage. Design cruise speed is set to 160 kn. While departure and arrival altitude is sea level, cruise altitude is 10,000 ft. As different propulsion concepts are likely to show unequal climb performance, the climb segment is carried out with a maximum possible climb angle. In contrast, the descent segment is flown following an identical pattern for all aircraft concepts. In addition to fuel and electric energy required to perform the design mission itself, fuel and electric energy for 45 minutes holding are considered during the sizing process. More precisely, the aircraft is assumed to climb to 1500 ft after a missed approach, perform the holding flight, descend to sea level, and land at the destination airport. Holding flight is carried out at 80% cruise speed.

For evaluation of the proposed powertrain concept's efficiency, a comparison with a generic, conventionally powered, reference aircraft configuration is carried out. This configuration features a high wing and a single engine. To ensure a fair and meaningful comparison between different concepts, the conventional aircraft is designed towards the same top-level aircraft requirements (TLARs). In addition, wherever applicable, identical design specifications are employed. Most importantly, for comparison of all aircraft configurations, the same design and evaluation methods are used. Thus, modeling inaccuracies have a smaller influence on the relative comparison between different concepts.

Initial sizing results based on requirements and design specifications as described above for the conventionally powered reference aircraft include a power loading of 13.6 lb/hp and a wing loading of 15.55 lb/sq. ft. A further execution of the MICADO sizing process results in an aircraft design with an empty mass of 1939 lb and a corresponding maximum takeoff mass of 3043 lb. Accordingly, calculated wing area is 117 sq. ft and engine power is 224 hp. While estimated block fuel consumption on the design mission comes to 266 lb, overall mission fuel demand including reserves for 45 minutes holding is 304 lb. The average fuel flow during cruise flight is 10.1 gph. A detailed mass breakdown can be found in Fig. 5. Aircraft structure mass including fuselage, wing, empennage and landing gear sums up to 883 lb. While the installed engine adds 563 lb, systems and furnishings add 493 lb to the empty weight.

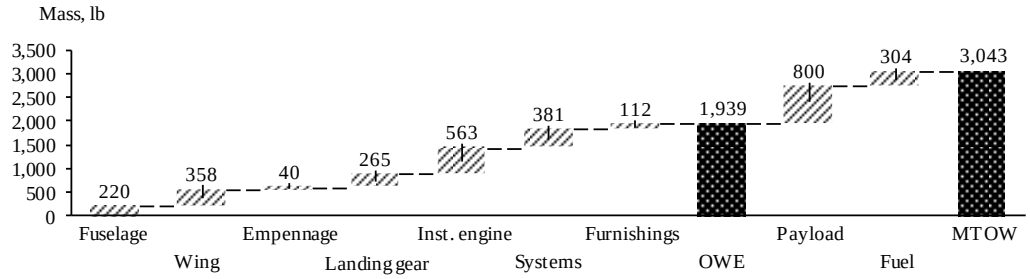

Fig. 5 Mass breakdown of conventional reference aircraft

As one aim of the application of the TTR-parallel powertrain is sizing the combustion engine to meet only cruise power demand, engine power output over mission distance is evaluated. An investigation for the design mission confirms that maximum engine power output is only required during takeoff and climb. After these two mission segments power output drops to around 69% rated power. During the cruise segment, power output of the engine constantly slightly decreases. A corresponding plot of engine power over mission distance is shown in Fig. 6.

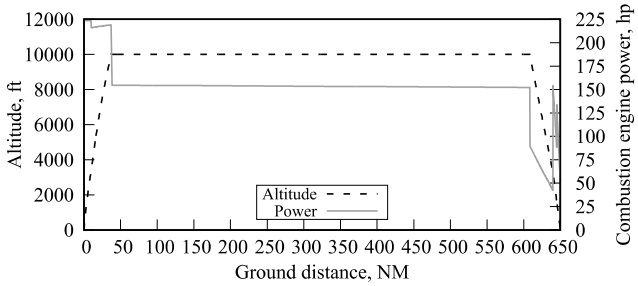

Fig. 6 Power output of cruise propeller engine over mission distance

III. Results and sensitivity analyses

Evaluation of aircraft concepts can be done with respect to several aspects, such as efficiency, economics or noise. In this study, the focus is on fuel and energy consumption while other aspects like costs or emissions play a subordinate role. For all aircraft configurations with DEP a lift drop due to the wing-mounted high-lift propeller nacelles is considered during the MICADO sizing iterations as described in chapter B. Due to uncertainties regarding the actual amount of this lift drop and the lack of high-fidelity CFD data or experimental results, all calculations are performed in the assumption of a constant lift drop of ΔC_L=0.1. In order to reflect the uncertainty, tendencies for less and more intense lift drops, i.e. ΔC_L=0.08 and ΔC_L=0.12, are given as well.

Sizing results for an aircraft with the proposed TTR-parallel powertrain architecture and meeting requirements and design specifications as described before reveal that this aircraft configuration is considerably heavier than the conventional reference. A mass breakdown for both aircraft concepts is displayed in Fig. 7. While estimated total mass of structure, systems and furnishings is smaller regarding the configuration with a TTR-parallel powertrain, weight savings resulting from a smaller combustion engine in this concept are overcompensated by additional electric powertrain components, such as electric motors and batteries. Studies regarding sensitivity in terms of the applied lift drop ΔC_L show maximum takeoff mass variations between 3305 lb and 3358 lb for ΔC_L=0.08 and ΔC_L=0.12, respectively.

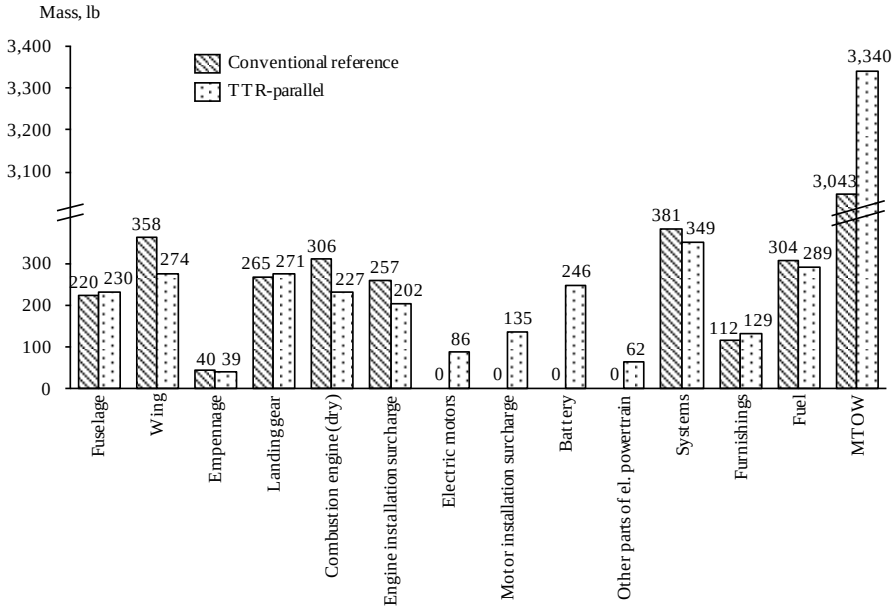

Fig. 7 Mass breakdown for conventional reference and aircraft with TTR-parallel powertrain

An investigation of the propulsive power demand over the duration of the mission shows that the sizing strategy for TTR-parallel powertrains can be successfully applied. In Fig. 8, the power output of combustion engine and electric motors over mission distance is given. In contrast to the conventional reference configuration, the combustion engine powering the cruise propeller of the new configuration is running at an almost constant level from takeoff to top-of-descent. Electrically driven high-lift propellers are only operated during takeoff, climb, and for final descent and landing. Based on TLARs and design specifications for the aircraft with the proposed TTR-parallel powertrain MICADO's *initial sizing* module returns a power loading of 12.7 lb/hp. With respect to the maximum takeoff mass of 3340 lb, overall installed engine power should be 261 hp. However, during the sizing loop it turns out that more overall installed power is necessary to implement the proposed powertrain concept successfully. While combustion engine power needs to be 166 hp to propel the aircraft during cruise flight, necessary combined power of all high-lift propeller motors is 157 hp (13.1 hp/motor) to provide necessary lift in low speed flight conditions. This is in total 323 hp.

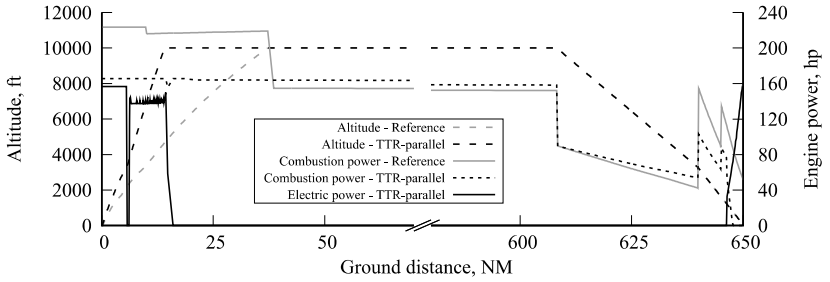

Fig. 8 Power output of cruise propeller engine and high-lift propeller motors (in total) over mission distance

Because of adding the DEP system, the combustion engine can be sized smaller with respect to rated power. In accordance with the assumption of a linear relationship between engine power and mass, the engine mass is smaller as well. This can be seen in the mass breakdown shown Fig. 7. While block fuel consumption for the reference aircraft on the design mission is 266 lb, the fuel consumption of the concept with DEP just slightly decreases to 253.7 lb, which is equivalent to -4.6%. In addition to hydrocarbon fuel, the aircraft with the hybrid parallel powertrain also requires 19.9 kWh of electric energy. If the uncertainty regarding the actual degree of interference between high-lift propeller nacelles and wing is considered, block fuel and electric energy demand vary between 249.3-257.7 lb fuel and 19.6-20.0 kWh electric energy for ΔC_L=0.08 and ΔC_L=0.12, respectively.

Since fuel and energy for a holding segment including additional climb and descent segments after a missed approached need to be considered for a proper sizing of both fuel tank and battery capacity, the battery capacity in

particular is significantly larger than the above-mentioned 19.9 kWh. Taking into account battery degradation and an assumed battery end-of-life when capacity has degraded to 90% rated capacity, required battery size is 27.9 kWh.

In addition to fuel and energy consumption, field performance and time-to-climb performance of the TTR-parallel powertrain layout is evaluated. The conventional reference aircraft requires 1190 ft ground run distance from brake release to lift-off. In contrast, the aircraft concept with DEP takes off after just 704 ft ground run at sea level and ISA conditions. This is due to the larger installed power and the resulting increased thrust. Because of the same reason, ground distance to climb is significantly lower for the concept with DEP as can be seen in Fig. 9. Accordingly, the DEP concept reaches cruise altitude around 7.5 minutes after takeoff while the conventional reference aircraft needs around 16.5 minutes. Estimated landing distance from screen height to full stop is around 2100 ft for both aircraft configurations as this parameter is less dependent on installed thrust.

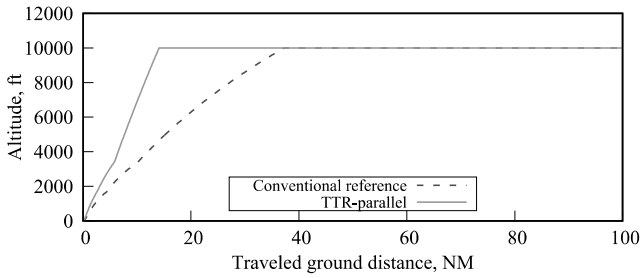

Fig. 9 Comparison of distance to climb

A. Sensitivity analyses

Regarding small aircraft with active lift augmentation by high-lift propellers, the design maximum high-lift coefficient has a major influence on aircraft design and characteristics. As described before in chapter II, wing area and size of active lift augmentation system components depend on this coefficient. Consequently, the influence of this design parameter is studied with respect to impact on aircraft design and performance. Starting from the baseline configuration's design maximum high-lift coefficient $C_{L,max,DEP} = 3.5$, the parameter is varied in steps of 0.25 within a range from 2.75 to 4. Results in terms of maximum takeoff mass, wing area, block fuel consumption, and block energy demand are shown in Fig. 10. It turns out that with increasing maximum high-lift coefficient the maximum takeoff mass constantly increases. Wing area reaches a local minimum at $C_{L,max,DEP} = 3.75$. However, both block fuel and block energy demand continuously increase with increasing maximum design high-lift coefficient. While block energy demand constantly increases with increasing design maximum high-lift coefficient, there is a minimum block fuel consumption for $C_{L,max,DEP} = 3.0$. In contrast to what might be expected, a more moderate application level of DEP technology increases its positive influence on fuel and energy consumption. Reasons for the efficiency increase due to smaller design high-lift coefficients are almost 50% less electric motor power requirement and a 30% smaller battery size if aircraft configurations with $C_{L,max,DEP} = 3.5$ and 3.0 are compared. Both aspects contribute to significant savings in component masses. The aircraft configuration with DEP and $C_{L,max,DEP} = 3.0$ requires 8.0% less fuel on the design mission than the conventional reference aircraft.

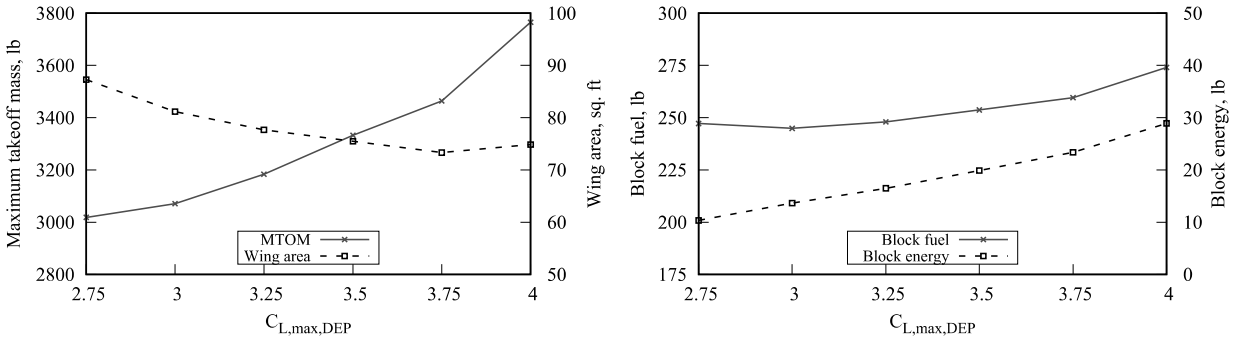

Fig. 10 Influence of design maximum high-lift coefficient on wing area, maximum takeoff mass, block energy, and block fuel consumption

In addition to the design maximum high-lift coefficient, past studies at ILR [2] revealed that cruise speed has a strong influence on the efficiency of small aircraft using DEP. For this reason, a sensitivity analysis regarding the

influence of cruise speed is carried out. Beginning with 160 kn design cruise speed of the baseline configuration, this parameter is altered in steps of 7.5 kn. Two steps in each direction are evaluated. For the smallest design cruise speed of 145 kn the sizing algorithm does not find a converging solution. Therefore, a further data point for a design cruise speed of 149 kn is added. Results shown in Fig. 11 indicate that for both aircraft configurations both maximum takeoff mass and wing area increase with increasing design cruise speed. Similarly, fuel consumption increases with increasing cruise speed. While block fuel consumption is always smaller for the aircraft concept with DEP, the difference is less distinct for smaller cruise speeds. In contrast to block fuel, the demand for block energy decreases slightly at higher cruise speeds. While rated power of high-lift propeller motors does not significantly depend on cruise speed, the size of the combustion engine driving the cruise propeller increases with increasing cruise speed. A more powerful cruise engine is the reason for shorter time to reach cruise altitude. Thus, high-lift propellers, which support in the climb segment, are operated for less time. Consequently, less electric energy is required.

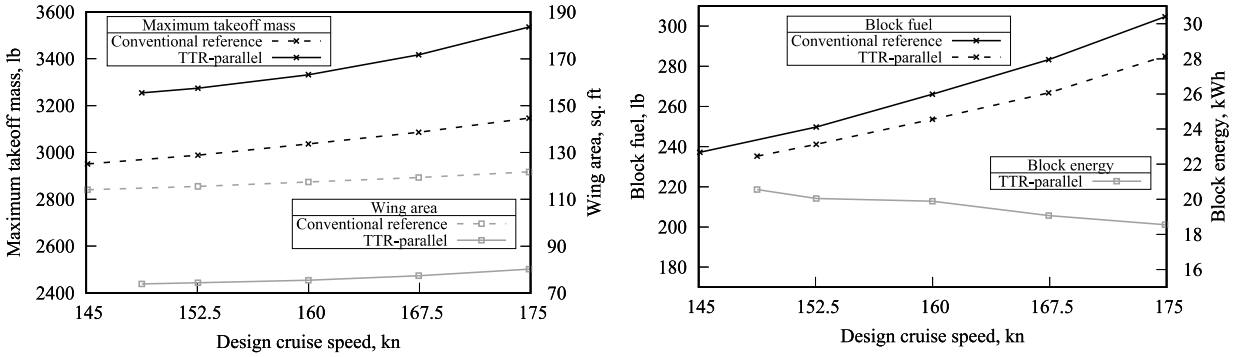

Fig. 11 Influence of cruise speed on wing area, maximum takeoff mass, block energy, and block fuel consumption

In addition to the analyses of the influence of individual parameter variations, a full parametric study including the simultaneous variation of design maximum high-lift coefficient and cruise speed is carried out. Similar to the sensitivity studies before, the influence of cruise speed is studied in steps of 7.5 kn and design maximum high-lift coefficient in steps of 0.25. Two steps in each direction are investigated. Results in terms of the parameter variation's influence on block fuel and block energy are presented in Fig. 12. The block fuel consumption of the conventional reference aircraft for investigated cruise speeds is included in the chart for comparison. Similar to the sensitivity analysis in terms of design cruise speed, the sizing algorithm does not find converged solutions for some parameter configurations. In more detail, high design maximum high-lift coefficients in combination with low design cruise speeds are infeasible.

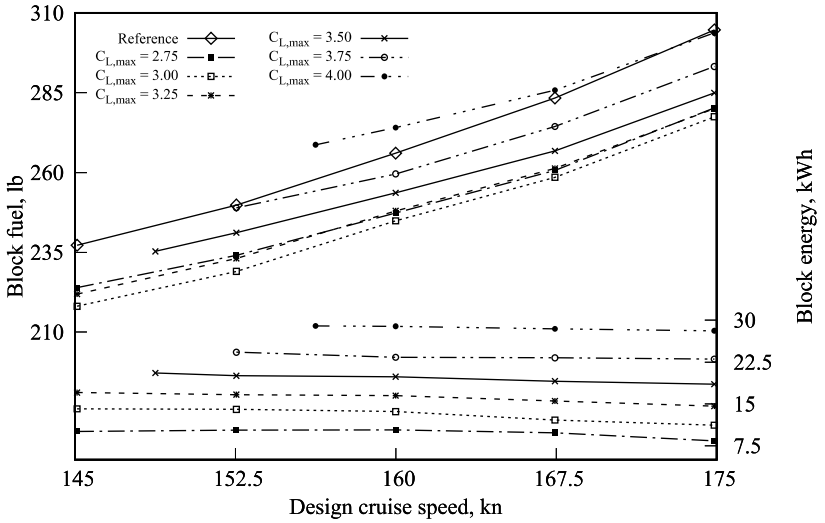

Fig. 12 Full parametric study results regarding the influence of cruise speed and maximum design high-lift coefficient on block fuel and block energy demand

Similar to the findings of the single parameter sensitivity studies, block fuel consumption on design mission increases for all investigated aircraft concepts with increasing cruise speed. This is true for both conventional and hybrid-parallel aircraft. In contrast to block fuel demand, block electric energy requirements decrease with increasing cruise speed for all investigated parameter combinations of the hybrid-parallel aircraft. A comparison to the fuel demand of the conventional reference configuration shows that not all hybrid-parallel configurations need less fuel on the design mission. In more detail, configurations with high design maximum high-lift coefficients in combination with low design cruise speeds turn out to be less fuel efficient than the generic conventional counterpart. Moreover, results of the full parametric study confirm the existence of an optimum design maximum high-lift coefficient. For all investigated parameter combinations a design maximum high-lift coefficient of $C_{L,max,DEP} = 3.0$ results in the lowest fuel consumption.

IV. Conclusion

Regarding the investigated design space, the comparison of aircraft performance in terms of fuel efficiency reveals a hydrocarbon fuel saving potential of up to 8%, i.e. around 21 lb, on the design mission if a TTR-parallel hybrid powertrain with DEP instead of a single conventional combustion engine is chosen to power a small aircraft. Additional electric energy is up to 25-30 kWh for less favorable TTR-parallel hybrid concepts. The most favorable design maximum high-lift coefficient for the TTR-parallel configuration in terms of fuel consumption is $C_{L,max,DEP} = 3.0$. Aircraft configurations with this lift coefficient require, in addition to fuel, around 14 kWh electric energy on the design mission, which equals an energy equivalent fuel amount of up to around 2.6 lb if an energy density of 5.4 kWh/lb (43 MJ/kg) is assumed. In total, equivalent primary energy consumption, i.e. fuel and electric energy, can be decreased by around 7%.

Since assumptions regarding the technological level of important components of the electric powertrain include an already available gravimetric battery energy density of 250 Wh/kg and a power-to-weight ratio of 3 kW/kg (1.82 hp/lb) for electric motors, an application of this concept seems possible in the near-term future. Any further technological progress, in particular with respect to gravimetric battery energy density, increases efficiency of the proposed powertrain concept. As huge technological progress is still necessary to build all-electric aircraft with comparable performance characteristics, the potential of the proposed TTR-parallel powertrain architecture can further increase in the meantime.

Although the TTR-parallel powertrain offers fuel saving potential compared to the conventional reference, unfavorable aspects of this configuration should be kept in mind. First, a complete additional powertrain is added to the aircraft. This adds extra weight, makes the system more complex and is likely to increase both engineering and production costs and thus acquisition costs of the aircraft. Second, additional components increase the workload during maintenance checks, which reflects in higher maintenance expenses as part of direct operating costs. Third, a battery is a component that experiences calendrical and cyclical degradation. This also adds to operating costs.

V. Outlook

Results of this study as well as findings in the literature underline the necessity of an appropriate consideration of the aerodynamic interaction between (high-lift) propeller nacelles and wings even at the stage of conceptual design. In this study, a simple model in terms of a penalty on the main wing's lift production performance is applied. A next step regarding a more precise consideration of nacelle-wing-interference in the context of conceptual design could be the calculation of response surfaces or derivation of lower order models returning the influence of high-lift propeller nacelles on lift and drag based on input parameters, such as wing properties, number of nacelles and nacelle properties, and operating condition. These response surfaces or lower order models should be based on a set of high-fidelity CFD calculations.

While technical feasibility of the TTR-parallel powertrain concept could be proven in this study, a comprehensive sustainability analysis is still pending. The corresponding economic viability evaluation should include, amongst others, estimations for acquisition costs of aircraft with hybrid-electric powertrains, additional maintenance efforts, and costs related with battery charging and degradation. Calculations regarding the ecological footprint should compare reduced emissions due to fuel savings to additional emissions originating from electricity production.

As mentioned in the introduction, not only the TTR-parallel hybrid powertrain represents a technically feasible solution for small aircraft with DEP in general, but also a serial-hybrid powertrain. Since this study revealed a hydrocarbon fuel saving potential of up to 13%, it seems worth comparing the performance of different hybrid-electric powertrain architectures for small aircraft with DEP.

Acknowledgments

The present studies have been carried out in the project Silent Air Taxi (SAT), funded by the German national research funding LuFo V (Luftfahrtforschungsprogramm). The authors would like to acknowledge the support of the German Ministry of Economics (BMWi).

References

[1] Borer, N. K., Patterson, M. D., Viken, J. K., Moore, M. D., Bevirt, J., Stoll, A. M., and Gibson, A. R., "Design and Performance of the NASA SCEPTOR Distributed Electric Propulsion Flight Demonstrator" *16th AIAA Aviation Technology, Integration, and Operations Conference,* American Institute of Aeronautics and Astronautics (AIAA), Washington, D.C, 2016. doi: 10.2514/6.2016-3920.

[2] Kreimeier, M., *Evaluation of On-Demand Air Mobility with Utilization of Electric Powered Small Aircraft*, Aachen, 2018.

[3] Thomson, R., Nazukin, M., Sachdeva, N., and Martinez, N., "Aircraft Electrical Propulsion - The Next Chapter of Aviation?: It is not a question of if, but when" Think:Act, 2017.

[4] Hepperle, M., "Electric Flight - Potential and Limitations" *Energy Efficient Technologies and Concepts of Operation,* NATO Science and Technology Organization, Lisbon, Portugal, 2012.

[5] Fraunhofer-Institut für System- und Innovationsforschung ISI, "Energiespeicher-Roadmap (Update 2017): Hochenergie-Batterien 2030+ und Perspektiven zukünftiger Batterietechnologien" Fraunhofer-Institut für System- und Innovationsforschung ISI, 2017.

[6] Risse, K., Anton, E., Lammering, T., Franz, K., and Hoernschemeyer, R., "An Integrated Environment for Preliminary Aircraft Design and Optimization" *53rd AIAA/ASME/ASCE/AHS/ASC Structures, Structural Dynamics and Materials Conference*, AIAA 2012-1675, American Institute of Aeronautics and Astronautics (AIAA), Honolulu, Hawaii, 2012. doi: 10.2514/6.2012-1675.

[7] Horstmann, K. H., Engelbrecht, T., and Liersch, C. M., "LIFTING_LINE: Version 2.5", 2016.

[8] Horstmann, K.-H., *Ein Mehrfachtraglinienverfahren und seine Verwendung für Entwurf und Nachrechnung nichtplanarer Flügelanordnungen*, Köln : Wiss. Berichtswesen d. DFVLR, Braunschweig, Germany, 1987.

[9] Patterson, M. D., *Conceptual design of high-lift propeller systems for small electric aircraft*, Dissertation, 2016.

[10] Veldhuis, L. L. M., *Propeller Wing Aerodynamic Interaction*, Delft, The Netherlands, 2005.

[11] Sadraey, M. H., *Aircraft design. A systems engineering approach*, Wiley, Chichestet, West Sussex, 2012.

[12] Deere, K. A., Viken, J. K., Viken, S. A., Carter, M. B., Wiese, M. R., and Farr, N., "Computational Analysis of a Wing Designed for the X-57 Distributed Electric Propulsion Aircraft" *35th AIAA Applied Aerodynamics Conference,* American Institute of Aeronautics and Astronautics (AIAA), Denver, Colorado, 2017.

[13] National Aeronautics and Space Administration (NASA), "About OpenVSP", URL: http://openvsp.org/learn.shtml [retrieved 4 May 2017].

[14] Drela, M., and Youngren, H., "Athena Vortex Lattice - AVL 3.36 User Primer" [online], 2017, URL: http://web.mit.edu/drela/Public/web/avl/.

[15] "Certification Specification 23 - Normal, Utility, Aerobatic and Commuter Aeroplanes" European Aviation Safety Agency (EASA), 2017.

[16] Roskam, J., *Airplane Design. Part V: Component Weight Estimation,* 1st edn., DARcorperation, Lawrence, Kansas, 1985.